

# Connecting the Navigational Clock to Sun Compass Input in Monarch Butterfly Brain

Ivo Sauman,<sup>2,5</sup> Adriana D. Briscoe,<sup>3,5</sup>  
Haisun Zhu,<sup>1</sup> Dingding Shi,<sup>1</sup> Oren Froy,<sup>1,6</sup>  
Julia Stalleicken,<sup>4,7</sup> Quan Yuan,<sup>1</sup>  
Amy Casselman,<sup>1</sup> and Steven M. Reppert<sup>1,\*</sup>

<sup>1</sup>Department of Neurobiology  
University of Massachusetts Medical School  
LRB – 728

364 Plantation Street  
Worcester, Massachusetts 01605

<sup>2</sup>Institute of Entomology  
Czech Academy of Sciences  
Ceske Budejovice  
Czech Republic

<sup>3</sup>Comparative and Evolutionary Physiology Group  
Department of Ecology and Evolutionary Biology  
University of California  
Irvine, California 92697

<sup>4</sup>VW Nachwuchsgruppe Animal Navigation  
Institute of Biology and Environmental Sciences  
University of Oldenburg  
D-26111 Oldenburg  
Germany

## Summary

Migratory monarch butterflies (*Danaus plexippus*) use a time-compensated sun compass to navigate to their overwintering grounds in Mexico. Although polarized light is one of the celestial cues used for orientation, the spectral content (color) of that light has not been fully explored. We cloned the cDNAs of three visual pigment-encoding opsins (ultraviolet [UV], blue, and long wavelength) and found that all three are expressed uniformly in main retina. The photoreceptors of the polarization-specialized dorsal rim area, on the other hand, are monochromatic for the UV opsin. Behavioral studies support the importance of polarized UV light for flight orientation. Next, we used clock protein expression patterns to identify the location of a circadian clock in the dorsolateral protocerebrum of butterfly brain. To provide a link between the clock and the sun compass, we identified a CRYPTOCHROME-staining neural pathway that likely connects the circadian clock to polarized light input entering brain.

## Introduction

Remarkable progress has been made in understanding the molecular and cellular basis of circadian clocks in

animals over the past decade (Stanewsky, 2002; Reppert and Weaver, 2002). One of the most intriguing functions of circadian clocks—their use in time-compensated sun compass navigation (von Frisch, 1967; Kramer, 1957)—has received only scant attention, however. From a functional vantage point, it is clear that time compensation is an absolute requirement for successful migration and, ultimately, survival, if celestial cues are used for long-distance navigation (Froy et al., 2003).

During their spectacular fall migration, North American monarch butterflies (*Danaus plexippus*) use a time-compensated sun compass to help them navigate to their overwintering sites in central Mexico (Perez et al., 1997; Mouritsen and Frost, 2002; Froy et al., 2003). Because this navigational capability is largely genetically determined (Brower, 1996), we are developing the monarch butterfly as a model to study the molecular and cellular basis of time-compensated sun compass navigation. Our ultimate goal is to understand the molecular and anatomical mechanisms for circadian clock interactions with the sun compass that enable migrants to maintain a fixed south/southwesterly flight bearing as the sun moves across the sky each day.

Previous studies suggest that monarch butterflies can use the angle of plane polarized light (e-vector) as an orientation (sun compass) cue (Hyatt, 1993; Reppert et al., 2004), and based on studies in hymenopterans (Brines and Gould, 1979; Edrich et al., 1979; Wehner, 1997), monarchs might also use the sun itself and/or spectral-intensity gradients. Because ultraviolet (UV) light is important for the initiation of oriented flight in monarch butterflies (Froy et al., 2003), it has been difficult to determine solely by behavioral assays whether polarized light in the UV range is important for orientation during sustained flight.

Like many insects (Labhart and Meyer, 1999), monarchs possess photoreceptors in the dorsal rim area (DRA) of the compound eye that are anatomically specialized for polarized-light detection (Reppert et al., 2004). Because the DRA of *Drosophila melanogaster* has a unique photoreceptor-specific pattern of opsin expression relative to the main retina (Wernet et al., 2003), we wondered whether a similar pattern of opsin expression occurs for the DRA of monarch butterflies.

Our previous work with monarch butterflies has also shown that disruption of the molecular circadian clockwork by constant light disrupts the time-compensated component of time-compensated sun compass orientation behavior (Froy et al., 2003). The molecular clock was monitored in that study by assessing the rhythmic expression of monarch *period* (*per*) mRNA levels in whole heads, because, as discussed below, *per* is an essential component of the circadian clock of *Drosophila*. It has not been known, however, where in monarch brain a circadian clock actually resides.

In *Drosophila*, the intracellular clock mechanism involves transcriptional feedback loops that drive persistent rhythms in mRNA and protein levels of key clock components (Stanewsky, 2002). The negative feedback

\*Correspondence: Steven.Reppert@umassmed.edu

<sup>5</sup>These authors contributed equally to this work.

<sup>6</sup>Current Address: Institute of Biochemistry, Food Science and Nutrition, Faculty of Agricultural, Food, and Environmental Quality, The Hebrew University of Jerusalem, P.O. Box 12, Rehovot 76100, Israel

<sup>7</sup>Practical work was done in the Comparative and Evolutionary Physiology Group, Department of Ecology and Evolutionary Biology, University of California, Irvine, California 92697.

loop involves the dynamic regulation of the *per* and *timeless* (*tim*) genes. The resultant PER and TIM proteins heterodimerize and translocate back into the nucleus where PER inhibits transcription. TIM appears to regulate PER protein stability and nuclear transport and is also necessary for photic responses that reset (entrain) the circadian clock (see Williams and Sehgal, 2001). Cryptochrome (CRY) is colocalized with PER and TIM and is a blue-light photoreceptor involved in photic entrainment (Emery et al., 1998; Stanewsky et al., 1998; Emery et al., 2000).

On the basis of the *Drosophila* clockwork, we reasoned that the evaluation of clock protein expression in monarch butterfly brain (e.g., the expression patterns of PER, TIM, and CRY) could reveal the location of a circadian clock involved in navigational activities. Indeed, in another lepidopteran, the Chinese oak silkworm *Antheraea pernyi*, PER and TIM are rhythmically expressed in brain in four large  $l_1$  neurons in each dorsolateral hemisphere that have been proposed to function as circadian clock cells (Sauman and Reppert, 1996). Interestingly, PER and TIM are primarily cytoplasmic throughout the 24 hr day in the silkworm neurons, whereas in *Drosophila* pacemaker neurons these proteins undergo temporally regulated nuclear transport that is critical for clock function (Stanewsky, 2002).

In the current report, we set out to provide a firm link between the circadian clock and the sun compass. First, we determined the pattern of opsin expression in the DRA photoreceptors of the monarch to identify the spectral content of polarized light that might be involved in flight orientation. We cloned three opsin-encoding cDNAs and ascertained that all three are expressed uniformly in the main retina. The DRA, on the other hand, expresses only the UV opsin. We complemented these anatomical findings with behavioral studies and found that polarized light in the UV range is important for flight orientation.

Next, we examined the expression profiles of PER, TIM and CRY to identify the location of a circadian clock in monarch butterfly brain. We found strong evidence for a brain clock in the dorsolateral protocerebrum. We found that a cryptochrome-containing neural pathway may connect the circadian clock to polarized light input entering the brain from the DRA of compound eye. Taken together, the results provide insights into a “navigational clock” and its connection to a sun compass in monarch butterfly brain.

## Results and Discussion

### Opsin Sequences and Phylogeny

Based on the wavelengths for peak sensitivity, rhodopsins expressed in the photoreceptors of the insect compound eye are classified as short wavelength (indicating a peak sensitivity of 300–400 nm), middle wavelength (400–500 nm) and long wavelength (LW, 500–600 nm). Molecularly, these physiological classifications correspond to three major clades of rhodopsin apoproteins (opsins): UV, blue, and LW. Our use of the term ‘opsin’ throughout this paper refers to opsins that are homologous to those found in the photoreceptors of the insect compound eye.

Using monarch head cDNA, we cloned the full-length cDNAs for three opsin genes, which, based on phylogenetic analyses, represent a UV opsin (*DpUVRh*, GenBank AY605546), a blue opsin (*DpBlueRh*, AY605544), and a long wavelength opsin (*DpLWRh*, AY605545) (see Figure S1 in the Supplemental Data available with this article online). The LW opsin likely has peak spectral sensitivity in the green (ca. 550 nm), based on study of the visual pigment absorption spectrum maxima of the closely related Queen butterfly, *Danaus gilippus* (Briscoe and Chittka, 2001). The monarch opsin cDNA sequences are highly homologous to the overlapping portions of the UV, blue, and LW (green) opsin mRNA transcripts that have been localized to the photoreceptor cells of the retina of *Vanessa cardui*, the only other butterfly of the family Nymphalidae so far examined (Briscoe et al., 2003) (data not shown).

The existence of only one LW opsin in these two nymphalid butterflies differs from the situation in butterflies of the family Papilionidae, which generally have several LW opsins expressed in retina (Briscoe, 2000) (Figure S1). In fact, phylogenetic analysis of the opsin gene family indicates that two duplications of an ancestral LW opsin gene occurred along the papilionid lineage (Briscoe, 2001). Importantly, the heterogeneous coexpression of filtering pigments with the LW opsin in monarch retina expands effectively the number of LW-sensitive receptors available for color vision (unpublished data). It is therefore likely that monarchs have tetrachromatic vision based primarily on three opsins and a lateral filtering pigment (also see below).

### Uniform Pattern of Opsin Expression in the Main Retina

The basic unit of the butterfly compound eye, the ommatidium, contains nine photoreceptor cells (R1–R9) that express the light-sensitive visual (opsin) pigments embedded in microvillous membranes of a fused rhabdom (Figure 1). The monarch photoreceptor cells are arranged in a semi-tiered fashion (Figure 1B), in which the cell bodies of the R1 and R2 cells are widest near the crystalline cone and then taper considerably as they approach the basement membrane. The tiny R9 cell sits just above the basement membrane. To study opsin expression in R1–R9 throughout the monarch eye, we made digoxigenin-labeled antisense riboprobes to the UTRs of the opsin cDNAs (to avoid cross-hybridization) and examined their pattern of hybridization on cryostat-sectioned tissue.

In situ hybridizations on semitangential sections and longitudinal sections through the whole retina revealed a uniform dorsal-to ventral distribution of *DpUVRh* and *DpBlueRh* mRNA expression (Figure S2). Examination of monarch retina cross-sections, longitudinal sections, and dissected ommatidia showed that *DpUVRh* mRNA expression in the main retina was restricted to the R1 and R2 photoreceptor cells (Figure 2A). A survey of 102 ommatidia of the lateral retina revealed that 17% showed *DpUVRh* mRNA expression in both R1 and R2, 54% showed expression in either R1 or R2, and 29% did not express *DpUVRh* mRNA. *DpBlueRh* expression was also restricted to R1 and R2, which did not overlap with *DpUVRh* expression (Figure 2, compare [A] and

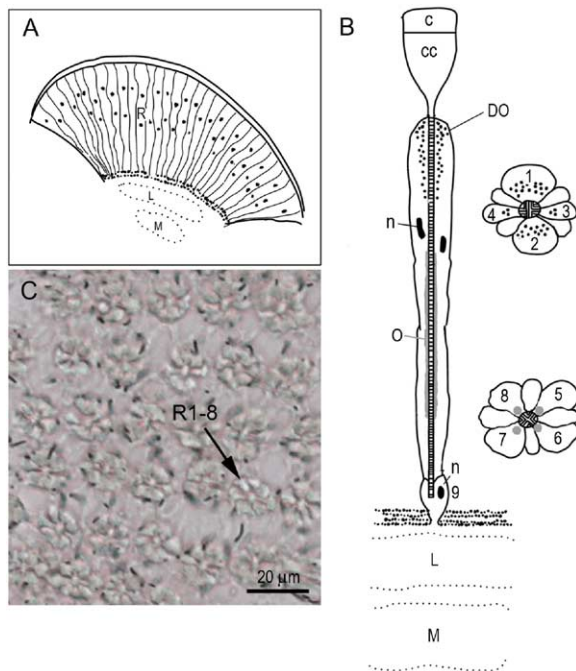


Figure 1. Anatomical Overview of the Compound Eye of the Monarch Butterfly

(A) Diagram of a longitudinal section through the compound eye. Black dots indicate the location of photoreceptor nuclei. R, retina; L, lamina; M, medulla.

(B) Schematic of a monarch ommatidium showing the R1–R9 photoreceptor cells in the main retina, as well as the presence of dark orange pupillary pigments (DO, black dots) that facilitate adaptation of the eye under different illuminant conditions. Heterogeneously expressed orange filtering pigments (O, gray line and circles) produce more than one spectral type of photoreceptor for long-wavelength light (unpublished data). Cross-hatched areas indicate the fused microvillous membranes of the rhabdomeres that contain the visual pigment protein. C, cornea; CC, crystalline cone; n, nuclei.

(C) DIC image of a tangential section of the retina showing the R1–R8 photoreceptor cells arranged in a radial fashion around the rhabdom.

[B]). A survey of 102 ommatidia of the lateral retina revealed that 27% showed *DpBlueRh* mRNA expression in both R1 and R2, 52% showed expression in either R1 or R2, and 21% did not express *DpBlueRh* mRNA (Figure 2B). These percentages suggest that the majority, if not all of the R1 and R2 cells in the main retina, express either *DpUVRh* or *DpBlueRh*. *DpLWRh* mRNA was expressed in photoreceptor cells R3 through R8 in all ommatidia of the main monarch retina, which was apparent in cross-sections, longitudinal sections, and dissociated ommatidia (Figure 2C, data not shown). The *DpLWRh* mRNA transcript was also detected in the apical R9 photoreceptor in dissociated ommatidia (data not shown).

Collectively, the expression patterns of the three opsin mRNAs in monarch main retina indicate nonoverlapping opsin expression in each photoreceptor cell. Furthermore, the mutually exclusive expression of the UV and blue opsin mRNAs in R1 and R2 photoreceptors gives rise to three types of ommatidia in the main ret-

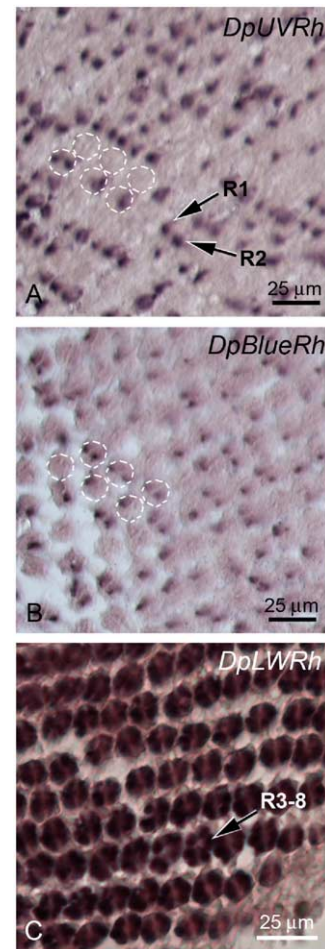


Figure 2. Opsin Expression in the Main Retina

(A) Tangential section of ommatidia (14  $\mu$ m) showing *DpUVRh* mRNA expression in R1 and R2 photoreceptor cells.

(B) Tangential section of ommatidia showing *DpBlueRh* mRNA expression in R1 and R2 that was nonoverlapping with *DpUVRh* expression. Dotted circles indicate identical ommatidia in adjacent sections.

(C) Tangential section showing *DpLWRh* mRNA expressed in the R3–R8 photoreceptor cells in all ommatidia in the main retina.

ina: those expressing the UV and LW opsins, those expressing the blue and LW opsins, and those expressing all three. The opsin expression patterns in monarch retina are similar to those in *Vanessa*, the only difference being the existence of a dorsoventral gradient in *Vanessa*; that is, the dorsal retina mainly consists of UV and LW opsin-expressing ommatidia (Briscoe et al., 2003).

The uniform dorsoventral distribution of UV and blue opsin expression in the main retina of monarch butterflies suggests that if skylight spectral-intensity gradients are used in sun compass orientation, the gradients would be sensed throughout the retina and would not be confined to a particular region.

#### The Dorsal Rim Area Expresses Only the UV Opsin

We next focused our studies of opsin expression on the DRA, which has ommatidia with rhabdomeres that are



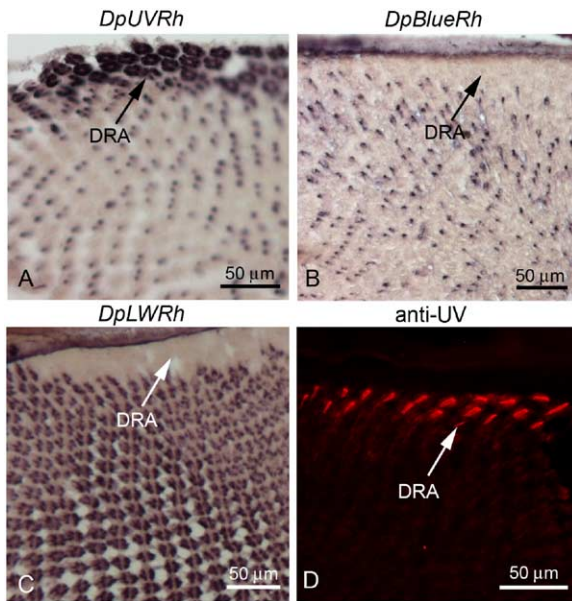


**Figure 3. Opsin Expression in the Dorsal Rim Area**  
 (A) Two to three rows of the ommatidia in the dorsal rim area (DRA) express *DpUVRh* mRNA in R1–R8 photoreceptor cells, in contrast to adjacent ommatidia, which express the *DpUVRh* mRNA in only the R1 and/or R2.  
 (B) Section adjacent to (A), showing the complete absence of *DpBlueRh* opsin mRNA expression in the DRA ommatidia and expression of the same transcript in R1 and R2 in adjacent retina.  
 (C) Section adjacent to (B), showing the complete absence of *DpLWRh* opsin mRNA expression in the DRA ommatidia and expression in R3–R8 in adjacent retina.  
 (D) Localization of the UV opsin protein in DRA by immunocytochemistry.

specialized for polarized-light detection (Reppert et al., 2004), to determine what spectral type of photoreceptor might be most important for detecting polarized skylight.

Strikingly, an area at the dorsalmost margin of the monarch eye stands out from the rest of the retina: cross-sections of this area showed that the R1 through R8 photoreceptor cells express only *DpUVRh* mRNA (Figure 3A). As observed in dissociated ommatidia, this strong expression is present throughout the entire length of the photoreceptor cells (not shown), although we were unable to determine conclusively that *DpUVRh* mRNA is expressed in R9 cells in the DRA. No *DpBlueRh* or *DpLWRh* mRNA was detected in the DRA ommatidia, though it is clearly present in the adjacent ommatidia of the main retina (Figures 3B and 3C). The DRA, as defined by these ommatidia expressing only the UV opsin, occurred within a distinct area 40 to 50 ommatidia in length and situated at the dorsal margin of the eye close to the antenna base. It is one to three ommatidia in depth from the eye margin (Figure 3A) and includes a total of approximately 100 ommatidia in each eye ( $n = 3$ ).

The DRA ommatidia also showed strong UV opsin immunoreactivity with prominent staining of the rhabdoms (Figure 3D). We noticed that the rhabdoms of these ommatidia are thicker in diameter and more in-

tensely immunostained than the rhabdoms of ommatidia in the main retina adjacent to the DRA (data not shown). This reflects UV opsin staining throughout the entire rhabdom because of UV opsin expression from all R1–R8 photoreceptor cells, compared to ommatidia in the rest of the retina in which the UV opsin is either not expressed (no immunofluorescence) or is expressed in only R1 and/or R2 photoreceptor cells (limited rhabdom staining). These variations in UV opsin staining in rhabdoms in main retina mirror our finding of UV opsin mRNA expression in ommatidia in main retina (Figure 2A). Because the rhabdoms of butterfly eyes are fused, it is difficult to distinguish by visual inspection of the pattern of rhabdom immunostaining those ommatidia with one versus two UV opsin-expressing cells.

Our assessment of opsin expression in the anatomically specialized DRA of monarch butterflies, which has previously been shown to contain orthogonally oriented microvilli (Reppert et al., 2004), indicates that all eight photoreceptor cells per ommatidium express only the UV opsin. Monochromatic receptors are required for efficient perception of polarized light in order to avoid interference with color information (Labhart and Meyer, 2002). DRA opsin expression has not been reported in any other butterfly.

### Polarized UV Light and Monarch Butterfly Orientation

We then examined the importance of polarized light in the UV range for monarch butterfly orientation by placing butterflies in a flight simulator outdoors and using a broad-band linear polarizing filter (HNP'B, transmission 275–750 nm), as previously described (Reppert et al., 2004). The butterflies were positioned below the polarizing filter so that the angle of skylight vision through the filter was restricted to 80° and the sun was not directly visible. We then used a transparent filter that blocks >95% of light transmission below 397 nm (UV-interference filter) to cover the top of the simulator barrel. As our previous studies have shown that rotation of the polarizing filter by 90° causes a corresponding change in flight direction (Reppert et al., 2004), butterflies were challenged with a 90° rotation of the polarizing filter, either with or without the UV-interference filter in place. If polarized UV light is important for monarch butterfly orientation, then UV interference should dampen or substantially alter the orientation response to the 90° rotation in the polarizing filter.

Four butterflies were examined at consecutive 5 min intervals of flight in the simulator. Each 5 min orientation pattern was plotted as a circular histogram, and virtual flight paths were constructed. Four sequential flight records were examined (see Figures 4A–4D): The first record recorded flight orientation before rotation of the polarizing filter, while the second recorded flight after a 90° rotation of the polarizing filter to obtain a “baseline” response to a 90° change in the polarization axis. Between the second and third records, the UV-interference filter was positioned above the butterflies prior to a second 90° rotation in the polarizing filter, and flight orientation was recorded for the third record (colored red). The fourth record recorded flight direction after removal of the UV-interference filter, but with no further rotation of the polarizing filter.

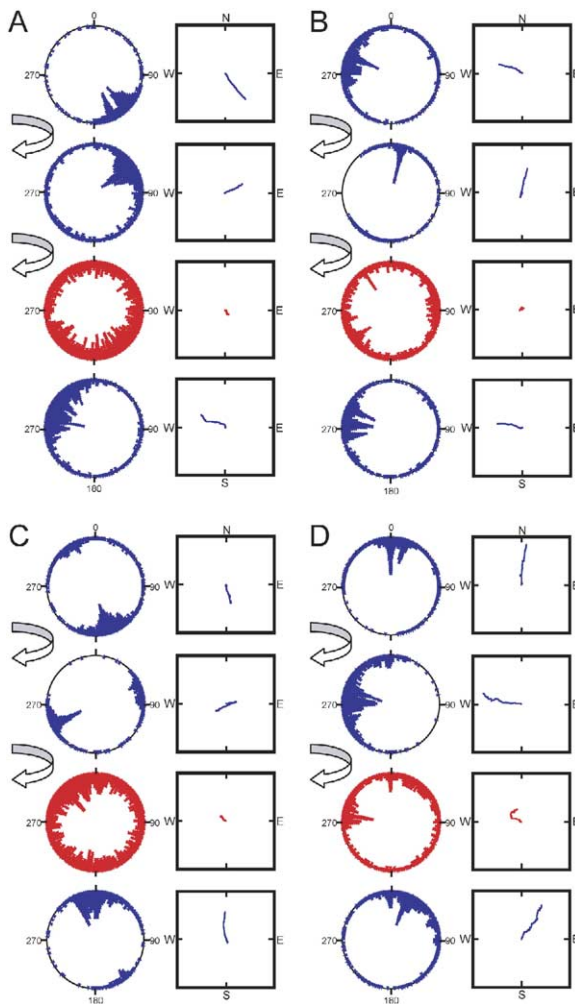


Figure 4. The Importance of Polarized UV Light for Flight Orientation

(A–D) Sequential records of flight orientation are shown as circular histograms in a column for each butterfly. All the butterflies started flight in the simulator with the polarizing filter plane placed parallel to the dominant skylight polarization axis viewed at the zenith. The polarization filter was rotated clockwise by 90° between each record of the top three records (curved arrows). Flight records in the presence of a UV-interference filter are colored red. The UV-interference filter was removed between the third and fourth record of each butterfly. Each circular histogram is a flight record of 5–7 min with sampling at 200 ms intervals. For each circular histogram, a calculated virtual flight path is depicted in the square to the right. We constructed virtual flight paths by starting in the center of the square and plotting each direction interval consecutively as one unit length (Mouritsen and Frost, 2002). 0° is North.

The baseline change in orientation induced by a 90° rotation of the polarizing filter was  $77.3^\circ \pm 3.8^\circ$  (mean  $\pm$  SEM,  $n = 4$ ) (Figures 4A–4D, two upper records). When the polarizing filter was rotated 90° again while UV-interference filter was applied, the orientation response was substantially altered (Figures 4A–4D, red highlighted records). Three of the butterflies exposed to the UV-interference filter showed at least a 70% decrease in directional flight (decreased length of the virtual flight paths in Figures 4A–4C, red flight paths) compared to

flight orientation without the UV-interference filter (virtual flight path lengths in the records above and below the red records). Video monitoring showed that this decrease was due to near-continuous circling behavior by the butterflies that was a mixture of flight and struggling without flight (Movie S1). This behavior produced the increase in nondirectional baseline activity seen in the circular histograms (Figures 4A–4C, red records) and contrasts with the continuous flight and intermittent circling observed when the UV-interference filter was not in place. It is noteworthy that the butterfly in Figure 4C manifested clear, within-record bimodal flight patterns, but with a dominant unimodal direction, without UV interference (Figure 4C, top, second, and fourth records), which is a behavioral response to a linear polarization axis (von Frisch, 1967; Waterman, 1981; Wehner, 2001). The fourth butterfly also manifested an altered orientation pattern in the face of UV interference (see red flight path of Figure 4D). This individual initially maintained the same flight direction as that before UV interference, but by the end of the UV-interference flight period, the butterfly had altered its orientation substantially. For all four butterflies, removal of the UV-interference filter, with no further change in the plane of the polarizing filter, resulted in sustained directional flight that shifted in orientation relative to the flight direction before UV interference (compare change in flight paths between the second and the lower records of Figures 4A–4D), consistent with the orientation position of the polarizing filter (mean response of  $109^\circ \pm 7.4^\circ$ ,  $n = 4$ ). Examination of the orientation positions for three of these butterflies when exposed to the UV-interference filter without altering the position of the polarizing filter indicated that exposure to the UV-interference filter itself does not cause large changes in orientation position (Figure S3).

Our behavioral data show that UV interference severely blunts or alters orientation responses to a change in the plane of skylight polarization. Taken together with the anatomical data, we propose that polarized light in the UV range, sensed through specialized DRA photoreceptors, is important for flight orientation in monarch butterflies. UV polarized light has been shown to be the best celestial cue for diurnal animals under partly cloudy conditions (while blue receptors are best at dawn and dusk) (Barta and Horvath 2004), which is consistent with monarchs' completely diurnal flight behavior and their tendency to cluster at dusk (Brower, 1996).

#### PER Staining Reveals Location of a Circadian Clock in Monarch Brain

How is information from DRA-derived polarized light input influenced by a circadian clock to produce time-compensated sun compass orientation? To begin to address this question, we sought to identify the location of a circadian clock in monarch brain that might be involved in navigational activities. This was approached by using PER immunocytochemistry to identify putative circadian clock cells. Two anti-PER antibodies (57/10w and 58/10w; Sauman and Reppert, 1996) were examined that gave identical staining patterns in monarch butterfly brain. The 58/10w antibody was used because of decreased background staining. There was consis-

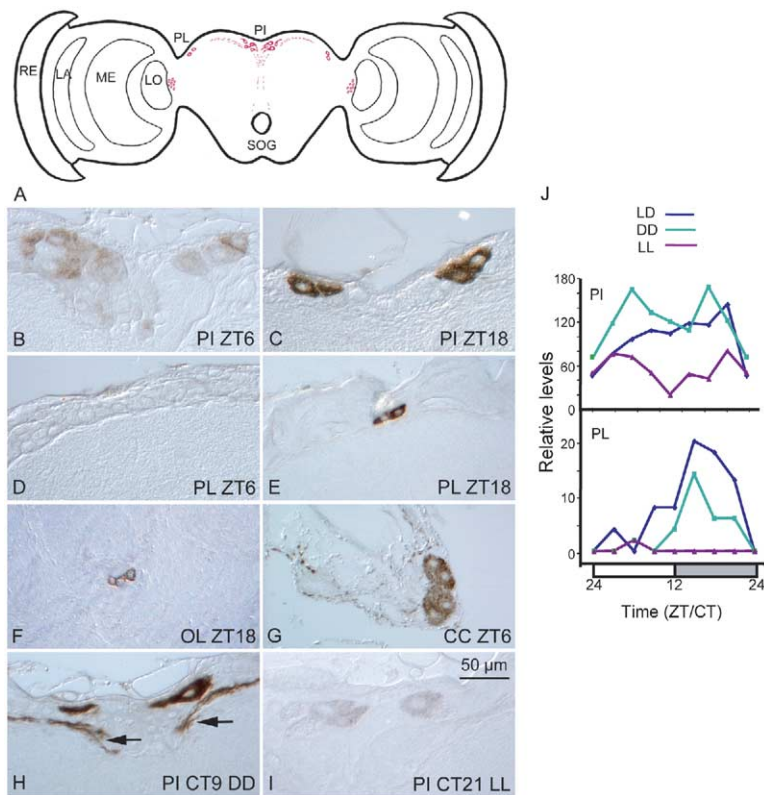


Figure 5. PER Immunoreactivity in Adult Monarch Brain

(A) Schematic diagram of a frontal section illustrating the topography of PER-immunoreactive cells. LA, lamina; ME, medulla; LO, lobula; PL, pars lateralis; PI, pars intercerebralis; SOG, subesophageal ganglion; RE, retina.  
 (B and C) PER staining in a group of large neurosecretory cells in PI at ZT 6 (B) and ZT 18 (C).  
 (D and E) Daily oscillation of PER immunoreactivity in two cells in PL at ZT 6 (D) and ZT 18 (E).  
 (F) A group of small PER-positive cells at the base of the OL at ZT 18.  
 (G) PER immunoreactive cells in corpus cardiacum (CC) at ZT 6.  
 (H) PER-positive cells and axonal projections (arrows) in PI in constant darkness (DD) at CT9.  
 (I) Decrease of PER staining intensity in the cells of PI in constant light (LL) at CT21.  
 (J) Semiquantitative assessment of PER immunostaining in PI or PL in LD, the second day in DD, and the second day in LL. Each value is the sum of cell intensity scores from three animals.

tent PER staining in a group of 8 to 12 large neurosecretory cells in the pars intercerebralis (PI) that was reduced during the day (compare Figures 5B and 5C) and in constant light (compare Figures 5H and 5I). These cells had stained axonal projections that projected laterally and ventrally (Figures 5A and 5H). There was also PER staining in two cells in the dorsolateral protocerebrum (pars lateralis, PL) of each hemisphere whose appearance was dependent on the phase of the 12 hr light:12 hr dark (LD) cycle examined; the stained cells were apparent at night (e.g., zeitgeber time [ZT] 18; Figure 5E), but were not detectable during the day (e.g., ZT 6; Figure 5D). Double-labeling experiments with both the anti-PER antibody and a monarch *per* cRNA probe demonstrated the colocalization of *per* transcript and protein in the same cells in both the PI and PL (data not shown). There was also PER staining in a group of small cells at the base of the optic lobe (Figure 5F) and in cells in the corpora cardiaca (Figure 5G); in the optic lobe the staining was variable, independent of the lighting conditions. In all cases, cellular staining was cytoplasmic. There was no detectable PER staining in the compound eye, in contrast to the situation in both *Drosophila* and *A. pernyi* (Stanewsky, 2002; Sauman and Reppert, 1996). The conspicuous lack of detectable retinal PER staining argues against the existence of circadian clocks in monarch photoreceptor cells. The same PER staining pattern in brain was seen in both summer and migratory butterflies.

Because of the variation in PER staining in the PI and PL over the LD cycle, we quantified PER staining in those regions at 3 hr intervals over a 24 hr period in LD,

constant darkness (DD), and constant light (LL). The daily oscillation in PER staining in the PI was broad in LD and did not persist in DD. In LL, there was an overall decrease in PER staining and no clear daily oscillation. In the PL, on the other hand, PER staining exhibited a robust 24 hr rhythm in LD, with peak staining at ZT 15. The rhythm in PER staining persisted in DD with a phase similar to that in LD, but the staining was eliminated at most times in LL.

The robust diurnal and circadian oscillation of PER staining in PL strongly suggests that a major circadian clock resides in these cells. We thus examined the expression of TIM staining in monarch brain by immunocytochemistry, as TIM should be coexpressed with PER in clock cells, on the basis of studies of *Drosophila* and *A. pernyi*. TIM-like immunoreactivity was detected in the cytoplasm of cells in the PI and in two cells in the PL of monarch brain, similar to the location of PER-positive cells (Figure S4). The modest intensity of TIM-like immunoreactivity in monarch brain together with high background levels, however, precluded definitive colocalization studies of PER/TIM staining and any assessment of oscillation in TIM staining in monarch brain.

#### CRY Staining in Monarch Brain

In *Drosophila* brain, all CRY-expressing cells also contain PER (Klarsfeld et al., 2004). In addition, CRY is a critical circadian photoreceptor in the fly (Emery et al., 2000). We therefore reasoned that PER and CRY should be colocalized in putative clock cells in monarch brain. We cloned the cDNA encoding monarch CRY (GenBank



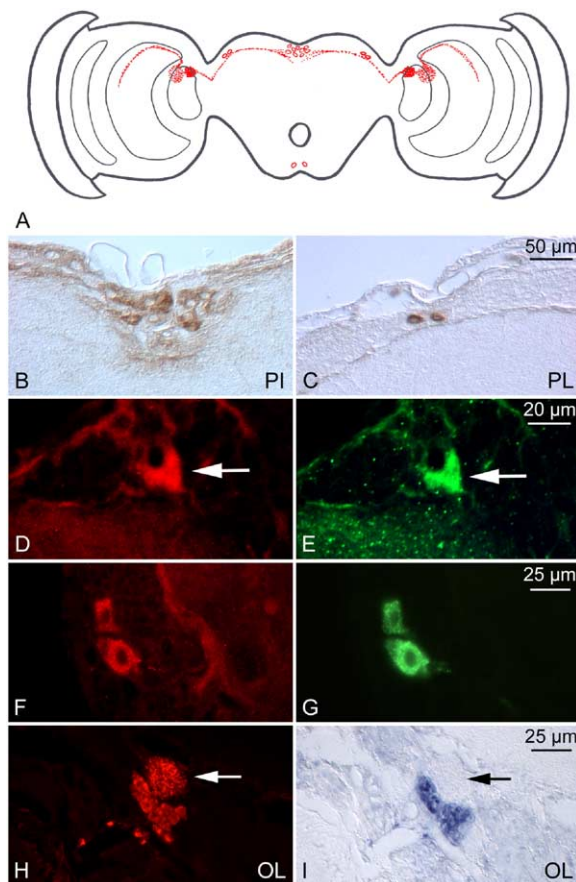


Figure 6. CRY Immunoreactive Cells and their Axonal Projections in Monarch Brain

- (A) Schematic representation of CRY-positive neurons and their axons.  
 (B) CRY staining in a restricted group of neurosecretory cells in pars intercerebralis (PI).  
 (C) CRY immunoreactivity in two cells in dorsolateral protocerebrum (PL).  
 (D and E) Double-labeling immunofluorescence of CRY (D) and PER (E) in the same cell (arrow) in PL.  
 (F and G) Double-labeling immunofluorescence of CRY (F) and COR (G) in the two cells in PL.  
 (H) A prominent group of small CRY-positive neurons in the dorsal region of the optic lobe (OL), forming a glomerular-like body of axonal projections (arrow).  
 (I) Brain section in (H) stained for the presence of *cry* mRNA demonstrates the colocalization of *cry* transcript and protein in the same cells. Note the absence of *cry* mRNA signal in the axonal projections forming the glomerular-like structure (arrow).

AAC83828; Figure S5) so that we could generate monarch-specific anti-CRY antibodies (Figure S6). Then, using immunocytochemistry we examined the anatomical distribution of monarch CRY expression and its relationship to PER-positive cells.

There was consistent CRY staining in a group of large neurosecretory cells in PI (Figure 6B); the intensity of staining did not vary with the lighting conditions (examined in LD, DD, and LL; data not shown). The CRY staining in PI appeared to be in the same location as cells staining for both PER and TIM immunoreactivity in PI. There was also CRY staining in two cells in the PL of

each hemisphere, the appearance of which was also independent of the lighting conditions (Figure 6C; data not shown). Moreover, double-labeling experiments with both the anti-CRY antibody and a monarch *cry* cRNA probe demonstrated the colocalization of the *cry* transcript and protein in the same cells in PL (data not shown). Importantly, double-labeling immunofluorescence revealed the colocalization of CRY and PER staining in the two cells in each PL (Figures 6D and 6E), as would be expected if these cells are indeed circadian clock cells in monarch butterfly brain.

The neuropeptide corazonin (COR), which appears to be involved in the initiation of ecdysis behavior (Kim et al., 2004), is co-expressed in the eight PER-positive cells in silkmoth brain previously proposed to function as circadian clock cells (Sauman and Reppert, 1996; Sauman and Hashimi, 1999; Qi-Miao et al., 2003; I. Sauman, unpublished data). PER-positive cells in the PL of the hawkmoth *Manduca sexta* that are homologous to the PER-positive cells in the silkmoth PL have been mapped as COR-expressing type-1a<sub>1</sub> neurosecretory cells (Wise et al., 2002). Thus, COR is a marker of lepidopteran 1a<sub>1</sub> neurosecretory cells that should label homologous neurons in monarch brain. Indeed, COR-immunoreactivity was expressed in four cells in each PL of butterfly brain (data not shown) and was colocalized in the two CRY/PER-positive cells in each PL (Figures 6F and 6G). This finding provides further evidence that these CRY/PER-positive cells in monarch brain are bona fide circadian clock neurons.

In addition to those in the PI and PL, there was a prominent group of small CRY-positive cells in the dorsal region of the optic lobe that formed a glomerular-like body with axonal projections (Figures 6H and 6I). No PER staining was found in this region (see Figure 5). Double-labeling experiments with both the anti-CRY antibody and the monarch *cry* cRNA probe demonstrated the colocalization of *cry* transcript and protein in the same cells in dorsal optic lobe (Figures 6H and 6I). As for PER, there was no detectable CRY staining in the monarch eye. Similar CRY staining patterns were seen in both summer and migratory butterflies.

### CRY Staining Reveals a Fiber Pathway from the Circadian Clock to the Optic Lobe

There were substantial CRY-immunoreactive fibers in the monarch brain (Figure 7) and, as discussed below, a CRY-containing pathway was delineated that could provide a vital link between the circadian clock in PL and axons originating from polarization-sensitive photoreceptors in the DRA. We identified CRY-positive fibers in the dorsolateral protocerebrum that were in direct contact with the two CRY-positive cells in PL (Figures 7A and 7B). This fiber pathway projected medially toward the PI and the protocerebral bridge and laterally toward the CRY-positive group of cells in the optic lobe. Fine projections from this optic lobe group of CRY-positive cells formed a glomerular-like arborization laterally from the cell bodies (Figures 6H and 7C). Additional CRY-positive fibers emanated from this glomerular structure and projected dorsolaterally along the surface of the medulla (Figure 7C). Finally, the fibers entered a posterior dorsal region of the medulla (sec-

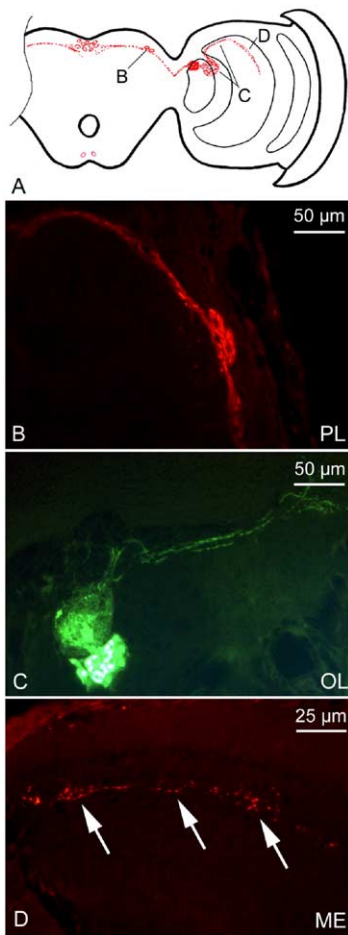


**Figure 7. CRY Immunoreactive Fibers in Monarch Brain**  
 (A) Schematic diagram depicting the topography of CRY immunoreactivity in the monarch brain.  
 (B) Two CRY immunofluorescent cells and CRY-positive fibers in dorsolateral protocerebrum (PL).  
 (C) A glomerular-like arborization of CRY-positive cells in the optic lobe (OL) and axons projecting toward the dorsolateral medulla.  
 (D) A fine arborization of CRY immunofluorescent fibers in the dorsolateral medulla (ME).

ond-order neuropil) and terminated as a fine varicose arborization in a single stratum of posterior dorsolateral medulla (Figure 7D).

Because the CRY-immunofluorescent fibers in the dorsolateral medulla are in the same location where axons from dorsal rim UV-expressing photoreceptors would be expected to project, on the basis of studies in flies (Hardie, 1984; Fortini and Rubin, 1991), we examined the relationship between the CRY-positive fibers and photoreceptor axons. This was evaluated by micro-injecting monarch DRA photoreceptor cells with fluorescent neuronal tracing dye.

We were able to show that the axons of these dorsal rim photoreceptors terminated in the posterior dorsolateral medulla of both summer and migratory butterflies. Although this was a consistent finding (in >40 injected animals), it was not seen following similar injection in the photoreceptor cells of more ventral or lateral ommatidia, which mostly terminated in the lamina (first-order neuropil). The injected dorsal rim photorecep-

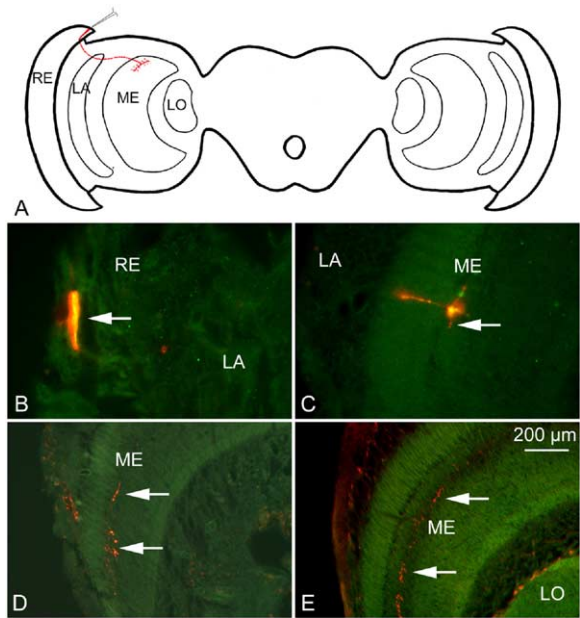


**Figure 8. Dorsal Rim Axonal Projections and their Relationship to CRY-Positive Fibers**  
 (A) Schematic illustration of the injected photoreceptor cell in the dorsal rim and its axonal projection into the dorsolateral medulla. RE, retina; LA, lamina; ME, medulla; LO, lobula.  
 (B) Injected dorsal rim area photoreceptor cell filled with fluorescent dye.  
 (C) Axonal projection from the injected photoreceptor cell entering the dorsolateral medulla (the second optic ganglion).  
 (D) Fine axonal arborization (varicose terminals) of the photoreceptor cell in the dorsolateral medulla.  
 (E) Fine axonal arborization of CRY-positive fibers in the dorsolateral medulla.

tors (Figures 8A and 8B) projected proximally through the dorsal region of the lamina. The dye-labeled projections then passed through a cell body layer (rind) between the first- and second-order neuropils relatively close to the dorsal surface of the optic lobe. They entered the medulla via its distal surface and finally terminated in a single layer (stratum) of the posterior dorsolateral medulla (Figures 8C and 8D). This represents the identical region of medulla in which the CRY-immunofluorescent fibers from the optic lobe CRY-positive cells terminated (Figures 7C and 8E). Due to an incompatibility of tissue processing for the two methods (dye injections and CRY immunofluorescence), we were not able to directly assess the likely colocalization of the CRY and photoreceptor cell terminals on the same brain section.

The anatomical data provide compelling evidence of a CRY-containing pathway that could communicate circadian information from the circadian clock neurons in PL to axons arising from polarization photoreceptors in the dorsal rim region of monarch eye. This pathway has not been described in any other insect, and it may be a hallmark feature of butterflies that use a time-compensated sun compass.

### Conclusions

The collective results provide strong evidence that a circadian clock important for monarch butterfly naviga-



tion resides in four cells in the dorsolateral region (PL) of monarch brain. The PER-positive cells in PI also appear to express TIM and CRY. It is thus possible that these cells contribute to the overall clock-regulated functions in monarch butterfly brain. In fact, studies in *Drosophila* have recently shown that the circadian network that controls locomotor behavior involves the activities of at least two distinct groups of circadian neurons (Stoleru et al., 2004; Grima et al., 2004). The lack of nuclear staining for PER and TIM seen in monarch brain has been found in most of the nondipteran insects that have been examined (Sauman and Reppert, 1996; Zavodskaya et al., 2003), emphasizing the need for more extensive analysis (Rosato and Kyriacou, 2001).

Our most provocative finding is the existence of a CRY-positive fiber pathway from the clock neurons in PL to the optic medulla in the same location where the axons from dorsal rim photoreceptors terminate. This pathway may provide a critical link between the circadian clock and sun compass input into brain. Electrophysiological studies of polarization-sensitive retinulae in dorsal rim ommatidia in eye and of polarization-sensitive neurons in the optic lobe in brain should clarify whether the CRY-containing pathway provides the relevant time-compensated information (Labhart and Meyer, 2002). It is also possible that there are multiple pathways that connect the circadian clock to different aspects of the sun compass system, including the sun compass itself (which may reside in the central complex; see Labhart and Meyer, 2002) and/or at the interface between the sun compass and the motor system.

The CRY-positive fiber pathway between PI and PL may also have an important function. The decreasing length of the day in the fall appears to be an important determinant for stimulating migratory behavior in butterflies (Goehring and Oberhauser, 2002). A defining characteristic of the migratory state is adult reproductive diapause (Brower, 1996), which contributes to an increased longevity necessary for survival at the overwintering grounds. Adult diapause is secondary to a deficiency in juvenile hormone (see Herman and Tatar, 2001), the synthesis of which is probably controlled by insulin-like peptides originating from neurosecretory cells in the PI. Therefore, a CRY-containing fiber pathway from the clock cells in the PL to the PI may play a vital role in providing photoperiodic information to the neuroendocrine system and, as mentioned above, involve secondary clocks in the PI itself.

## Experimental Procedures

### Animals

"Summer" butterflies were reproductively active and were purchased from commercial sources throughout the year. To confirm the clock protein staining patterns in brain in migratory butterflies, animals were captured near Eagle Pass, Texas, from October 10–12, 2004 and shipped to Worcester. The migratory females were dissected under 10× magnification to determine reproductive status, and all were found to be in reproductive diapause (indicated by the absence of mature oocytes). All butterflies were housed in the laboratory with controlled temperature (21°C for summer butterflies and 18°C for migrants), humidity (70%), and lighting. The butterflies were fed 10%–15% sucrose.

### Cloning and Sequence Analysis

cDNA fragments were cloned by degenerate polymerase chain reaction (PCR). cDNA templates for PCR were prepared from RNA

purified from monarch butterfly brains or whole heads. The ends of the coding regions were obtained by rapid amplification of cDNA ends (RACE; Clontech). Complete open reading frames were obtained by PfuTurbo (Stratagene) PCR from cDNA. Clones were sequenced at core facilities at the University of Massachusetts Medical School. Sequence analysis was facilitated by software from the Genetics Computing Group (GCG) and the National Center for Biotechnology Information website (<http://www.ncbi.nlm.nih.gov/BLAST/>).

### Phylogenetic Analysis

To explore the possibility that we had recovered members of all paralogous opsin genes from *Danaus plexippus*, we searched the only currently available lepidopteran genome resource, the *Bombyx mori* 3X (Mita et al., 2004) and 6X (Xia et al., 2004) assemblies in GenBank using the tBlastx search tool and whole genome sequence (wgs) setting. Full-length opsin cDNAs were downloaded, and the translated amino acids were aligned, using the ClustalW algorithm (Figure S1). Only first and second nucleotide positions were used in the tree reconstruction, as a test for composition homogeneity amongst lineages (Kumar and Gadagkar, 2001) was rejected for third positions (data not shown). The neighbor-joining algorithm with Tamura-Nei distance estimates with complete deletion of gaps was implemented in MEGA 3.0 (Kumar et al., 2004). Bootstrap analysis was performed using 500 replications.

### Antibody Production

For generating monarch CRY antibodies, purified protein containing the C-terminal 113 amino acids of monarch CRY was used as an immunogen in rats and guinea pigs, as previously described (Lee et al., 2001). Antisera were affinity purified and designated DpCRY-1-R and DpCRY-1-GP ("R", raised in rats; "GP", raised in guinea pigs). Both anti-CRY antibodies gave identical results when used for either immunocytochemistry or for probing Western blots (Figure S6). Western blotting was performed as described previously (Lee et al., 2001). The V-5 antibody used for Western blots was a monoclonal mouse anti-V5 IgG purchased from Invitrogen.

### Immunocytochemistry

Eye tissue was fixed as described in Briscoe et al. (2003), and cryostat-sectioned (14–16 μm slices). Prior to antibody incubation, the sections were washed in 100% cold acetone for 5 min, then washed for 30 min in 1× PBS, and finally washed for 5 min in 1× PBS/0.5% SDS. Dissected brain-suboesophageal ganglion complexes of adult monarchs were immediately processed for immunocytochemistry as described elsewhere (Sauman and Reppert, 1996). Stained sections were examined with the aid of the Zeiss Axioplane 2 or an Axioskop 2 plus microscope equipped with Nomarski (DIC) optics, epifluorescence, and a CCD camera.

The antibodies used for immunocytochemistry included: rabbit anti-*PgIRh5* (UV), (1:200; Briscoe and Nagy, 1999; Lampel et al., 2005); rabbit anti-*A. pernyi* PER (57/10w at 1:500 and 58/10w at 1:500; Sauman and Reppert, 1996); rabbit anti-CORAZONIN (from Makio Takeda; dilution, 1:1000), rat-TIM (307; from Michael W. Young; dilution, 1:1000) and anti-DpCRY-1-R and anti-DpCRY-1-GP. A Cy3-conjugated goat anti-rabbit secondary antibody (1:1000; Jackson Immuno Research Laboratories, Inc., West Corore, PA) incubated for 1–2 hr at room temperature was used to detect the anti-UV primary antibody.

To verify the specificity of immunological reactions, primary antibodies were replaced with normal goat serum. In additional controls of binding specificity, the anti-PER antibody and the anti-CORAZONIN antibody were preincubated with 100 molar excess of the respective original antigen prior to immunocytochemical staining. In all cases, no significant staining above background was observed.

### In Situ Hybridization

Fragments of monarch *DpUVRh*, *DpBlueRh*, *DpLWRh*, and *per* and *cry* cDNAs were subcloned into pCR II vector (Invitrogen) and used as templates for antisense and sense (control) digoxigenin (DIG)-labeled riboprobe synthesis. The riboprobe yield was assessed by dot blots.

For the opsin in situ hybridizations, the fixation and detection

methods are as described in [Briscoe et al. \(2003\)](#). For *per* and *cry*, the methods were similar except that after fixation in paraformaldehyde, the tissue was embedded in paraplast and sectioned (10  $\mu$ m). In situ hybridization was carried out using the mRNA locator kit (Ambion). The riboprobes were localized by incubation with an alkaline phosphatase-conjugated anti-digoxigenin antibody (Boehringer and Mannheim; 1:500 dilution overnight at 4°C) and visualized with BCIP and NBT (Perkin Elmer). DIG-labeled sense RNA probes were used in control experiments. In all cases, no signal was detected above background.

For double-labeling experiments, hybridized sections were incubated simultaneously with anti-DIG antibody and anti-PER or anti-CRY overnight at 4°C and detected with a fluorophore-conjugated secondary antibody (1 hr at RT). The AP activity was detected as described above.

For scoring of immunoreactive intensities, stained sections were coded and viewed under a microscope. Levels of staining were subjectively scored with an intensity scale ranging from 0 to 5 per cell. The time of collection was decoded after scoring.

#### Microinjections

Alexa Fluor-conjugated dextran neuronal tracer (10,000 MW, 10% in sterile water; Molecular Probes) was injected into photoreceptors of the dorsal rim area of CO<sub>2</sub>-anesthetized butterflies. For the injections, a glass microcapillary was inserted through a small opening made in the eye cuticle with a tungsten needle. The opening was sealed with silicone grease after the injection with the fluorescent tracers. Injected animals were kept in constant darkness for two days. Brains with eyes were dissected, fixed in paraformaldehyde, and processed as described for immunocytochemistry.

#### Behavioral Experiments

Monarch butterflies migrating through Massachusetts were captured in the wild in the fall of 2003 and 2004. The migrants were housed outside in plastic mesh cages with free access to 10% sucrose in water. Butterflies were tethered as previously described ([Mouritsen and Frost, 2002](#)), and flight behavior was monitored using a modified Mouritsen and Frost flight simulator as described ([Reppert et al., 2004](#)). The four individuals studied were part of a group of 13 butterflies that initially flew under the parallel-placed polarizer in the southwesterly (migratory) direction, when corrected for bimodal orientation ( $\alpha = 19^\circ/199^\circ$ ,  $n = 13$ ,  $r = 0.49$ ,  $p < 0.05$ ).

The linear polarizing filter was rotated by hand. The UV-interference filter was a long-wavelength pass filter with a photopic luminous transmission of 84% (E420 from Gentex, Carbondale, PA). Transmission values were as follows: 5%  $\geq$  397 nm; 50% = 420  $\pm$  6 nm; 80%  $\leq$  436 nm. Data in each orientation histogram were analyzed to determine the significance of orientation and the mean direction using circular statistics ([Batschelet, 1981](#)).

#### Supplemental Data

Supplemental data include six figures and a movie and can be found with this article online at <http://www.neuron.org/cgi/content/full/46/3/457/DC1/>.

#### Acknowledgments

We thank Choogon Lee for producing the monarch anti-CRY antibodies; David R. Weaver for suggestions; Aditi V. Chavda, Lawrence Lee, Kasia Macko, Marilou Sison-Mangus, and Guillermo Zaccardi for assistance; Steve A. Kay for reagents; Makio Takeda and Michael W. Young for antibodies; and Carol Cullar for supplying migratory butterflies. J.S. contributed to the opsin expression parts of the paper. This work was supported in part by NIH grant R01 NS047141 (S.M.R.); GAAVCR grant A5007205 (I.S.); NSF grant IBN-0346765 (A.D.B.); and a German Academy Exchange Service Grant (DAAD) and the Volkswagenstiftung to J.S.

Received: January 10, 2005

Revised: March 2, 2005

Accepted: March 16, 2005

Published: May 4, 2005

#### References

- Barta, A., and Horvath, G. (2004). Why is it advantageous for animals to detect celestial polarization in the ultraviolet? Skylight polarization under clouds and canopies is strongest in the UV. *J. Theor. Biol.* 226, 429–437.
- Batschelet, E. (1981). *Circular Statistics in Biology* (New York: Academic Press.).
- Brines, M.L., and Gould, J.L. (1979). Bees have rules. *Science* 206, 571–573.
- Briscoe, A.D. (2000). Six opsins from the butterfly *Papilio glaucus*: molecular phylogenetic evidence for multiple origins of red-sensitive visual pigments in insects. *J. Mol. Evol.* 51, 110–121.
- Briscoe, A.D. (2001). Functional diversification of lepidopteran opsins following gene duplication. *Mol. Biol. Evol.* 18, 2270–2279.
- Briscoe, A.D., and Chittka, L. (2001). The evolution of color vision in insects. *Annu. Rev. Entomol.* 46, 471–510.
- Briscoe, A.D., and Nagy, L. (1999). Spatial expression of opsins in the retina and brain of the tiger swallowtail *Papilio glaucus*. *Am. Zool.* 39, 254B.
- Briscoe, A.D., Bernard, G.D., Szeto, A.S., Nagy, L.M., and White, R.H. (2003). Not all butterfly eyes are created equal: Rhodopsin absorption spectra, molecular identification and localization of ultraviolet-, blue-, and green-sensitive rhodopsin-encoding mRNAs in the retina of *Vanessa cardui*. *J. Comp. Neurol.* 458, 334–349.
- Brower, L.P. (1996). Monarch butterfly orientation: missing pieces of a magnificent puzzle. *J. Exp. Biol.* 199, 93–103.
- Edrich, W., Neumeyer, C., and Helversen, O. (1979). “Anti-sun orientation” of bees with regard to a field of ultraviolet light. *J. Comp. Physiol.* 134, 151–157.
- Emery, P., So, W.V., Kaneko, M., Hall, J.C., and Rosbash, M. (1998). CRY, a *Drosophila* clock and light-regulated cryptochrome, is a major contributor to circadian rhythm resetting and photosensitivity. *Cell* 95, 669–679.
- Emery, P., Stanewsky, R., Helfrich-Forster, C., Emery-Le, M., Hall, J.C., and Rosbash, M. (2000). *Drosophila* CRY is a deep brain circadian photoreceptor. *Neuron* 26, 493–504.
- Fortini, M.E., and Rubin, G.M. (1991). The optic lobe projection pattern of polarization-sensitive photoreceptor cells in *Drosophila melanogaster*. *Cell Tissue Res.* 265, 185–191.
- Froy, O., Gotter, A.L., Casselman, A.L., and Reppert, S.M. (2003). Illuminating the circadian clock in monarch butterfly migration. *Science* 300, 1303–1305.
- Goehring, L., and Oberhauser, K.S. (2002). Effects of photoperiod, temperature, and host plant age on induction of reproductive diapause and development time in *Danaus plexippus*. *Ecol. Entomol.* 27, 674–685.
- Grima, B., Chelot, E., Xia, R., and Rouyer, F. (2004). Morning and evening peaks of activity rely on different clock neurons of *Drosophila* brain. *Nature* 431, 869–871.
- Hardie, R.C. (1984). Properties of photoreceptors R7 and R8 in dorsal marginal ommatidia in the compound eyes of *Musca* and *Calliphora*. *J. Comp. Physiol. [A]* 154, 157–165.
- Herman, W.S., and Tatar, M. (2001). Juvenile hormone regulation of longevity in the migratory monarch butterfly. *Proc. R. Soc. Lond. B. Biol. Sci.* 268, 2509–2514.
- Hyatt, M.B. (1993). The use of polarization for migratory orientation by monarch butterflies. PhD thesis, University of Pittsburgh, Pittsburgh, Pennsylvania.
- Kim, Y.-J., Spalovska-Valachova, I., Cho, K.-H., Zitnanova, I., Park, Y., Adams, M.E., and Zitnan, D. (2004). Corazonin receptor signaling in ecycosis initiation. *Proc. Natl. Acad. Sci. USA* 101, 6704–6709.
- Klarsfeld, A., Malpel, S., Michard-Vanhee, C., Picot, M., Chelot, E., and Rouyer, F. (2004). Novel features of cryptochrome-mediated

- photoreception in the brain of the circadian clock of *Drosophila*. *J. Neurosci.* *24*, 1468–1477.
- Kramer, G. (1957). Experiments on bird orientation and their interpretation. *Ibis* *99*, 196–227.
- Kumar, S., and Gadagkar, S.R. (2001). Disparity index: a simple statistic to measure and test the homogeneity of substitution patterns between molecular sequences. *Genetics* *158*, 1321–1327.
- Kumar, S., Tamura, K., and Nei, M. (2004). MEGA3: integrated software for molecular evolutionary genetics analysis and sequence alignment. *Brief. Bioinform.* *5*, 150–163.
- Labhart, T., and Meyer, E.P. (1999). Detectors for polarized skylight in insects: a survey of ommatidial specializations in the dorsal rim area of the compound eye. *Microsc. Res. Tech.* *47*, 368–379.
- Labhart, T., and Meyer, E.P. (2002). Neural mechanisms in insect navigation: polarization compass and odometer. *Curr. Opin. Neurobiol.* *12*, 707–714.
- Lampel, J., Briscoe, A.D., and Wasserthal, L.T. (2005). Expression of UV-, blue-, long wavelength-sensitive opsins and melatonin in extraretinal photoreceptors of the optic lobes of hawkmoths. *Cell Tissue Res.*, in press.
- Lee, C., Etchegaray, J.-P., Cagampang, F.R.A., Loudon, A.S.I., and Reppert, S.M. (2001). Posttranslational mechanisms regulate the mammalian circadian clock. *Cell* *107*, 855–867.
- Mita, K., Kasahara, M., Sasaki, S., Nagayasu, Y., Yamada, T., Kanamori, H., Namiki, N., Kitagawa, M., Yamashita, H., and Yasukochi, Y. (2004). The genome sequence of silkworm, *Bombyx mori*. *DNA Res.* *11*, 27–35.
- Mouritsen, H., and Frost, B.J. (2002). Virtual migration in tethered flying monarch butterflies reveals their orientation mechanisms. *Proc. Natl. Acad. Sci. USA* *99*, 10162–10166.
- Perez, S.M., Taylor, O.R., and Jander, R. (1997). A sun compass in monarch butterflies. [letter]. *Nature* *387*, 29.
- Qi-Miao, S., Tanaka, S., and Takeda, M. (2003). Immunohistochemical localization of clock proteins (DBT and PER), and [His<sup>7</sup>]- and [Arg<sup>7</sup>]-corazonins in the cerebral ganglia of *Bombyx mori*: are corazonins down-stream regulators of circadian clocks? *Eur. J. Entomol.* *100*, 283–286.
- Reppert, S.M., and Weaver, D.R. (2002). Coordination of circadian clocks in mammals. *Nature* *418*, 935–941.
- Reppert, S.M., Zhu, H., and White, R.H. (2004). Polarized light helps monarch butterflies navigate. *Curr. Biol.* *14*, 155–158.
- Rosato, E., and Kyriacou, C.P. (2001). Flies, clocks and evolution. *Philos. Trans. R. Soc. Lond. B Biol. Sci.* *356*, 1769–1778.
- Sauman, I., and Hashimi, H. (1999). Insect clocks: what are they telling us besides time? *Entomol. Sci.* *2*, 589–596.
- Sauman, I., and Reppert, S.M. (1996). Circadian clock neurons in the silkworm *Antheraea pernyi*: novel mechanisms of period protein regulation. *Neuron* *17*, 889–900.
- Stanewsky, R. (2002). Genetic analysis of the circadian system in *Drosophila melanogaster* and mammals. *Cell Tissue Res.* *309*, 111–147.
- Stanewsky, R., Kaneko, M., Emery, P., Beretta, B., Wager-Smith, K., Kay, S.A., Rosbash, M., and Hall, J.C. (1998). The *cry<sup>b</sup>* mutation identifies cryptochrome as a circadian photoreceptor in *Drosophila*. *Cell* *95*, 681–692.
- Stoleru, D., Peng, Y., Agosto, J., and Rosbash, M. (2004). Coupled oscillators control morning and evening locomotor behavior of *Drosophila*. *Nature* *431*, 862–865.
- von Frisch, K. (1967). *The Dance Language and Orientation of Bees* (Cambridge, MA: Belknap Press of Harvard University Press).
- Waterman, T. (1981). Polarization sensitivity. In *Handbook of Sensory Physiology, Vision in Invertebrates*, H. Autrum, ed. (New York: Springer-Verlag), pp. 281–469.
- Wehner, R. (1997). The ant's celestial compass system: spectral and polarization channels. In *Orientation and Communication in Arthropods*, M. Lehner, ed. (Basel: Birkhauser Verlag), pp. 145–185.
- Wehner, R. (2001). Polarization vision—a uniform sensory capacity? *J. Exp. Biol.* *204*, 2589–2596.
- Wernet, M.F., Labhart, T., Baumann, F., Mazzoni, E.O., Pichaud, F., and Desplan, C. (2003). Homothorax switches function of *Drosophila* photoreceptors from color to polarized light sensors. *Cell* *115*, 267–279.
- Williams, J.A., and Sehgal, A. (2001). Molecular components of the circadian system in *Drosophila*. *Annu. Rev. Physiol.* *63*, 729–755.
- Wise, S., Davis, N.T., Tyndale, E., Noveral, J., Folwell, M.G., Bedian, V., Emery, I.F., and Siwicki, K.K. (2002). Neuroanatomical studies of period gene expression in the hawkmoth, *Manduca sexta*. *J. Comp. Neurol.* *447*, 366–380.
- Xia, Q., Zhou, Z., Lu, C., Cheng, D., Dai, F., Li, B., Zhao, P., Zha, X., Cheng, T., Chai, C., et al. (2004). A draft sequence for the genome of the domesticated silkworm (*Bombyx mori*). *Science* *306*, 1937–1940.
- Zavodskaya, R., Sauman, I., and Sehgal, F. (2003). Distribution of PER protein, pigment-dispersing hormone, prothoracicotropic hormone, and eclosion hormone in the cephalic nervous system of insects. *J. Biol. Rhythms* *18*, 106–122.